



An LP1 analogue, selective MOR agonist with a peculiar pharmacological profile, used to scrutiny the ligand binding domain



Simone Ronsisvalle^{a,*}, Giuseppina Aricò^a, Federica Panarello^a, Angelo Spadaro^a, Lorella Pasquinucci^a, Maria S. Pappalardo^a, Carmela Parenti^b, Nicole Ronsisvalle^c

^a Department of Drug Sciences, Medicinal Chemistry Section, University of Catania, Viale A. Doria 6, 95125 Catania, Italy

^b Department of Drug Sciences, Pharmacology and Toxicology Section, University of Catania, Italy

^c Department of Biomedical and Biotechnological Sciences, University of Catania, Italy

ARTICLE INFO

Article history:

Received 19 May 2016

Revised 26 August 2016

Accepted 27 August 2016

Available online 30 August 2016

Keywords:

MOR agonists

6,7-Benzomorphan scaffold

Modeling studies

Radioligand competition-binding assay

Tail-flick test

GPI and MVD assays

ABSTRACT

The hypothesis that central analgesia with reduced side effects is obtainable by occupying an 'allosteric' site in the MOR ligand binding domain requires the development of new ligands with peculiar pharmacological profile to be used as tools. New benzomorphan derivatives, analogues of LP1, a multitarget MOR agonist/DOR antagonist, were designed to examine in depth MOR ligand binding domain. Compound **5**, bearing a diphenylic *N*-substituent on the benzomorphan nucleus, showed an affinity ($K_i^1 = 0.5 \pm 0.2$ nM) comparable to that of LP1 and a better selectivity versus DOR and KOR. It elicits antinociceptive effects in ex vivo (GPI) and in vivo. This new compound engages receptor amino acidic residues not reached by LP1 and by other established MOR ligands. Molecular modeling studies, conducted on **5** and on several reference compounds, allowed us to propose possible residues in the MOR ligand binding domain essential for their interactions with 'orthosteric' and 'allosteric' binding sites.

© 2016 Elsevier Ltd. All rights reserved.

1. Introduction

Opioid analgesics are still the most commonly used drugs for the treatment of acute and chronic pain, from moderate to severe.^{1,2} They are considered to produce analgesia through three GPCRs, named μ -opioid receptor (MOR), δ -opioid receptor (DOR) and κ -opioid receptor (KOR)^{3,4}, which are activated by several endogenous opioid peptides.^{5,6} All these peptides are characterized by an N-terminal Tyr residue and morphine analogues, because of their stereo-specific interaction with the receptors, have always been considered peptidomimetics and its site of action considered the orthosteric binding site.

The search for safer and more effective analgesic drugs was initially oriented to the synthesis of high affinity and selective compounds toward each of receptor subpopulations^{6–8} with the main objective of understanding their physiological role^{9–14} and to separate antinociceptive activity from side effects. Several 'new' opioids were developed and some of them are in clinical use, but none is devoid of undesirable effects.^{15,16,4,17}

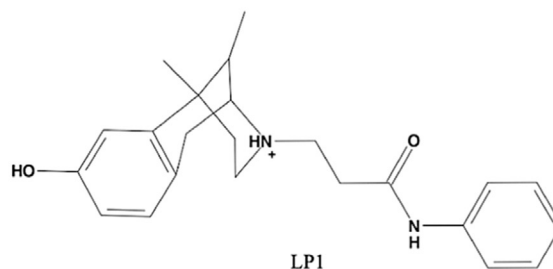
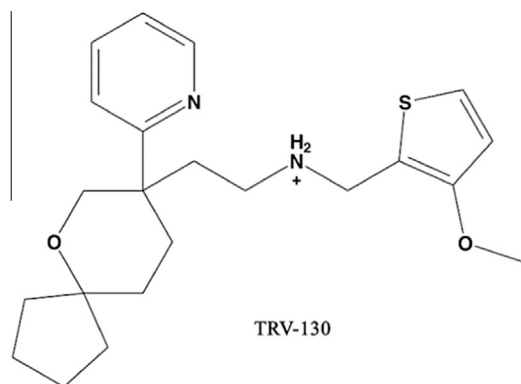
Several clinical studies showed that both side effects and antinociceptive action are mainly mediated through MOR^{14–16,4,17} and to take that in account, some researchers proposed the

existence of two different MOR subpopulations (MOR1 and MOR2).⁹ It was suggested that they could differentially mediate analgesic response and unwanted respiratory depression.^{18,19} However, only one μ receptor has been cloned so far and the ablation of a single receptor gene, i.e. *oprm1*, eliminates all MOR responses.^{20–23,16,24}

From the same perspective, a number of researchers reported that GPCRs can form dimers or oligomers and the MOR/DOR heterodimer attracted a lot of attention. Opioids combining MOR agonist–DOR antagonist activity may in fact be effective antinociceptive agents being able to attenuate MOR-mediated side effects.^{25–29} In a previous paper, we showed that the multitarget MOR agonist–DOR antagonist LP1, 3-[(2*R*,6*R*,11*R*)-8-hydroxy-6,11-dimethyl-1,4,5,6-tetrahydro-2,6-methano-3-benzazocin-3(2*H*)-yl]-*N*-phenylpropanamide, is a central acting antinociceptive agent with low potential to induce tolerance and potentially useful for persistent pain conditions.^{28,30,31} In contrast, the activation of DOR with MOR–DOR compounds led to the co-internalization and co-degradation of both MOR and DOR, allowing to hypothesize that the physiological dissociation of MOR from DOR signaling in the pain pathway could enhance MOR-mediated analgesia and reduce the associated side effects.³² Nevertheless, the co-expression of MOR and DOR receptors in a single cell is still controversial.³²

* Corresponding author. Tel.: +39 0957384209.

E-mail address: s.ronsisvalle@unicat.it (S. Ronsisvalle).



Recently, Suh³³ and Virk³⁴ clearly showed the complexity of the opioid receptor complex and that different biochemical mechanisms are simultaneously possible after receptor activation.^{35,36} The development of TRV-130 allowed DeWire et al.¹⁴ to hypothesize that MOR may signal through at least two distinct pathways mediated not only by G proteins but also based on β -arrestin recruitment. At the MOR, β -arrestins seem to act as negative modulator of analgesia and positive modulator of some side effects, desensitizing a GPCRs mediated signaling and stimulating independent cell signaling outcomes.¹⁴

Based on the above considerations, the development of opioid analgesics devoid of side effects clearly requires a better characterization of the MOR ligand binding domain (LBD) in order to identify compounds able to specifically activate physiological signaling pathways perhaps interacting with an allosteric binding site rather than with the morphine orthosteric binding site.

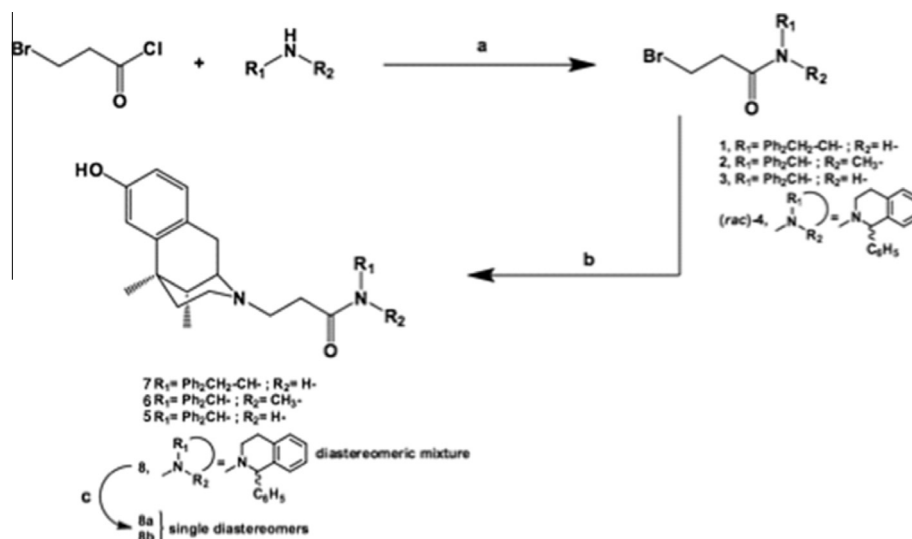
To identify molecular probes that allow to study the different mechanisms of receptor activation, we designed some new LP1 analogues **5–8**, **8a** and **8b**. Linear and rigid 3-diphenylalkyl-amide *N*-substituted normetazocine derivatives have been synthesized. Bulkier fragments were chosen to reduce DOR interaction. We report their binding affinities and ex vivo and in vivo pharmacolog-

ical properties of the most MOR selective compound. Molecular dynamic studies in comparison with some reference ligands were performed to identify binding interactions and to clarify structural requirements for orthosteric and allosteric binding.^{37,38}

2. Results and discussion

2.1. Chemistry

cis-(–)-(1*R*,5*R*,9*R*)-*N*-Normetazocine was separated from a commercially available racemic mixture as reported by Brine et al.³⁹ Compounds **1–4** were prepared by acylation of respective amines with bromoacetyl chloride in anhydrous THF at 0 °C (30 min) and at rt (30 min) in argon atmosphere. Racemic mixture (*rac*)-**4** was obtained using (*RS*)-1-phenyl-1,2,3,4-tetrahydroisoquinoline as starting amine. The *N*-substituted *cis*-(–)-*N*-normetazocine derivatives **5–8** were obtained by alkylation of *cis*-(–)-*N*-normetazocine in anhydrous MeOH with the respective bromoamide derivatives **1–4**. The alkylation procedure was performed in the dark under argon atmosphere in anhydrous MeOH at 50 °C using NaHCO₃ and KI. The diastereomeric mixture **8** was separated by HPLC into its diastereomers **8a** and **8b** in milligram amounts by multiple



Scheme 1. Synthetic route to target compounds **5**, **6**, **7**, **8**, **8a**, **8b**. Reagents and conditions: (a) TEA, dry THF, 0 °C 30 min/rt 30 min, argon; (b) *cis*-(–)-(1*R*,5*R*,9*R*)-*N*-normetazocine, NaHCO₃, KI, dry MeOH, 24 h, argon, dark; (c) diastereomeric HPLC separation (Chiralpak AD-H column, 90:10 v/v hexane/2-propanol).

repetitive injections under overload conditions on a Chiralpak AD-H analytical column (Scheme 1).

2.2. Biological activity

2.2.1. In vitro radioligand binding assay

Binding affinities of new compounds were evaluated by radioligand competition-binding assays in HEK293, CHO human and rat cells. The results of these experiments on compounds **5**, **6**, **7**, **8** and **8a,b** are summarized in Table 1. Compounds **5** ($K_i^H = 0.5$) and **6** ($K_i^H = 160$) demonstrate to have a good affinity and selectivity for MOR. Compound **7** showed a reduced affinity ($K_i^H = 84$), but is still selective for MOR. Compounds **8a** and **8b**, synthesized to analyze possible stereospecific interaction of the fragment with receptor, showed a reduced affinity with respect to **5**, while **6**, which with its methyl group mimics the piperidine fragment, showed a binding affinity comparable to **8**. Compound **5** showed a binding affinity similar to LP1 with a stronger μ/δ selectivity. Compound **5** was selected for further pharmacological studies.

2.2.2. In ex vivo pharmacology

Pharmacological activities were evaluated in vitro using isolated guinea pig ileum (GPI) to establish their agonist/antagonist functional activity.

Compound **5** caused a concentration dependent inhibition of electrically-evoked contractions of the guinea-pig isolated ileum

segments (pD_2 6.8 ± 0.05). As shown in Figures 1–3, the pre-treatment with Naloxone ($1 \mu\text{M}$), a non-selective opioid receptor antagonist, Naloxonazine ($1 \mu\text{M}$), a selective μ -opioid receptor antagonist or norbinaltorphimine (norBNI) ($1 \mu\text{M}$), a κ -selective opioid receptor antagonist failed to affect 5-induced inhibition of neurogenic contractions (control pD_2 6.8 ± 0.05 ; naloxone pD_2 6.4 ± 0.08 ; naloxonazine pD_2 6.5 ± 0.1 ; norBNI pD_2 6.9 ± 0.07).

The selective MOR agonist DAMGO concentration dependently inhibited the electrically induced contraction. The potency (pD_2) of **5** was similar to that of DAMGO (5 pD_2 6.8 ± 0.05 ; DAMGO pD_2 6.2 ± 0.08) (Fig. 4) and the association of the two compounds led to a slight increase of the inhibition of the electrically-evoked contractions (5-DAMGO pD_2 7.0 ± 0.06) (Fig. 4).

Compound **6** determined a concentration dependent inhibition of electrically-evoked contractions of the guinea-pig isolated ileum segments (pD_2 5.7 ± 0.08). As shown in Figure 5, in contrast to what was obtained with **5**, a single concentration (10^{-6} M) of Naloxone displaced to the right the concentration–response curve of **7** with a pD_2 of 4.1 ± 0.2 (Fig. 5).

2.2.3. In vivo pharmacology

Compound **5** was further tested to evaluate its antinociceptive effects in the mouse tail flick test. As shown in Figure 6 (panel A), **5**, in dosage range from 2.5 up to 10 mg/kg intraperitoneally injected (ip), increased tail flick latency (TFL) in a dose-dependent manner, with significant values at 30 min of observation. As shown

Table 1
Binding affinities of synthesized compounds*

Compd	MOR (K_i , nM)	KOR (K_i , nM)	DOR (K_i , nM)	K_i ratio κ/μ	K_i ratio δ/μ
5	0.5 ± 0.2	190 ± 0.13	440 ± 0.1	380	880
6	160 ± 0.09	370 ± 0.09	1400 ± 0.4	2.31	8.75
7	84 ± 0.1	680 ± 0.13	2900 ± 0.3	8.09	34.52
8 (\pm)	96 ± 0.1	ND	ND	ND	ND
8a	470 ± 0.1	1900 ± 0.3	7900 ± 1.7	4.04	16.8
8b	380 ± 0.1	900 ± 0.1	2900 ± 0.6	12.5	34.95
LP1	0.83 ± 0.05	110 ± 6	29.01 ± 1	132.5	33.8
TRV-130**	6 ± 1.7	$<10,000$	ND	1666.67	ND
DPDPE	ND	ND	1.7 ± 0.9	ND	ND
U-50488	ND	0.6 ± 0.7	ND	ND	ND
DAMGO	0.6 ± 0.6	ND	ND	ND	ND

ND not determined.

* The values are the means \pm SEM of three independent experiments. K_i values were obtained as [^3H]DAMGO displacement for the MOR, [^3H]DPDPE displacement for the DOR receptor, and [^3H]U69,593 displacement for the KOR receptor.

** [^3H]Diprenorphine 14.

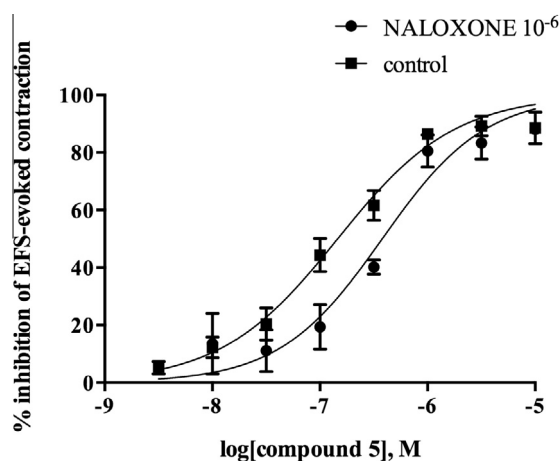


Figure 1. Effects of **5** in the electrically stimulated guinea pig ileum in the absence and presence of naloxone (10^{-6} M). Data represent means \pm SEM of 6–8 separate experiments.

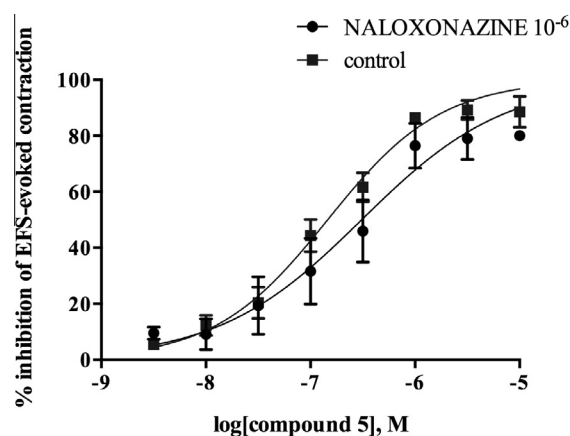


Figure 2. Effects of **5** in the electrically stimulated guinea pig ileum in the absence and presence of naloxonazine (10^{-6} M). Data represent means \pm SEM of 6–8 separate experiments.

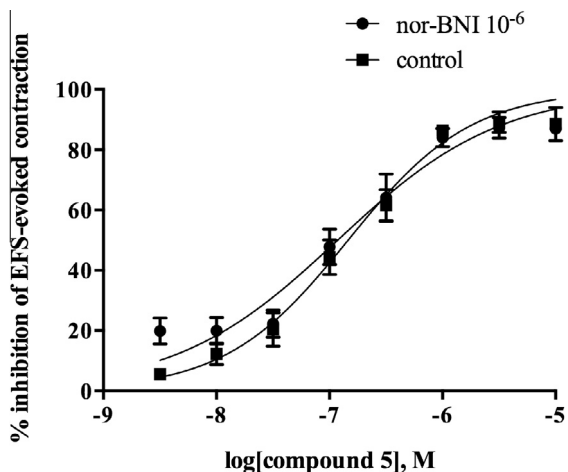


Figure 3. Effects of **5** in the electrically stimulated guinea pig ileum in the absence and presence of nor-BNI (10^{-6} M). Data represent means \pm SEM of 6–8 separate experiments.

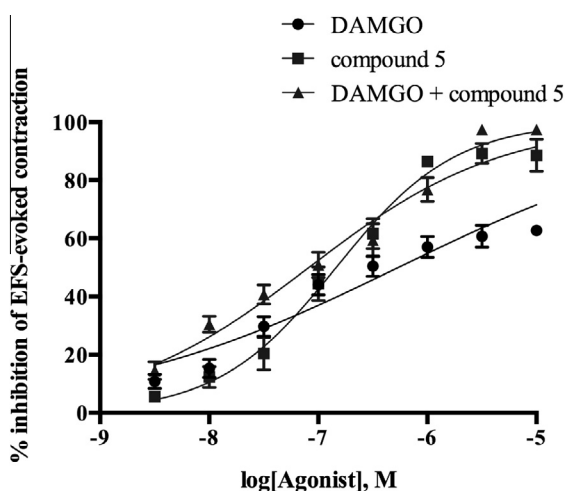


Figure 4. Effects of DAMGO and **5** in the electrically stimulated guinea pig ileum. Data represent means \pm SEM of 6–8 separate experiments.

in panel B (Fig. 6), **5** and morphine showed a similar potency at the dose of 5 mg/kg ip, but morphine maintained its antinociceptive effect until 60 min of observation ($^*P < 0.05$ vs saline treated-mice, $^{**}P < 0.05$ vs saline treated-mice).

Pretreatment with naloxone (3 mg/kg ip), 45 min prior to **5** (5 mg/kg ip), decreased the antinociceptive effect of the compound, confirming the interaction with opioid receptors in vivo (Fig. 7).

2.3. Molecular modeling studies

Ability to resolve X-ray of MOR, DOR and KOR receptors was a fundamental step toward the comprehension of protein conformational changes and to study protein activation cascades and activation or modulation of internalization processes.

MOR, DOR and KOR receptors crystals were presented in 2012 by Manglik et al. (PDB code 4DKL, resolution: 2.8 Å),⁴⁴ Granier et al. (4EK4)³⁶ and Wu et al. (4DJH),⁴⁰ respectively. Recently, another MOR crystal was published by Huang et al. (PDB code 5C1M, resolution: 2.1 Å).⁴¹

Molecular modeling studies on compounds **5–7** were first performed. In line with its binding data, compound **5** demonstrates to have the best docking score (-10.6) compared to **6** and **7**, which

show a docking score of -8.4 and -7.2 , respectively. Compounds **8a** and **8b** present similar values (-7.7 and -7.4).

In the dynamic studies their positions in the Ligand Binding Domain (LBD) were carefully evaluated. Most recurring interactions are observed with some second extracellular loop (ECL 2) amino acids, such as aspartic acid (Asp216), with the Cys217–Cys140 residues, which form the disulfide bond between ECL2 and the third transmembrane domain, and with asparagine in the 3rd transmembrane domain (TM) (Asn127) (Fig. 12).

In addition to the above mentioned amino acids, all compounds in the series show an interesting arene–arene interaction between the tyrosines in the 6th (Tyr299) and 7th (Tyr326) transmembrane domains and their diphenyl portion, likewise important, because it stabilizes the molecules in the LBD. These tyrosines seem to work like a gate allowing or not the reaching of Asp147 (3rd TM) binding region, the purporting morphine binding site (Fig. S1).

Trying to understand why compound **5** carried particular pharmacological results, we compared it with morphine but also with other established fully agonist ligands, such as DAMGO, LP1 and TRV-130.^{42–44,30,45,46}

Morphine shows a clear interaction with Asp147, confirming the results obtained by a number of researchers.^{42–44,30} Specifically, it establishes a hydrogen bond between the protonated nitrogen moiety and the carboxylic portion of Asp147, and interactions with Ile144 and Asn127 with its phenolic portion. The interaction with Asp147 is stable for all the 20 ns calculated by dynamic simulations (Fig. 8). As observed in Figure S6, the distance between His297 and the phenolic portion is always higher than 19 Å.

Moreover, some similarities between **5** and morphine are evident. Infact, looking at the RMSD of transmembrane I–III, both compounds are able to activate the same conformational changes (Fig. S2a–c). Nevertheless, morphine provokes an RMSD reduction on TM4, in comparison with the free protein. Opposite, **5** completely prevents this variability (Fig. S2d–f). It is possible to observe a morphine-like evolution with DAMGO (Fig. 9a–c). On TM6, morphine and DAMGO both influence the RMSD spectra in the same mode. Therefore, they could be able to promote similar biological effects on MOR. Compound **5**, however, provokes a strong stabilization of TM4 caused by its interaction with ECL2 amino acids.

Even more interesting resulted the evaluation of ligands RMSD (Fig. 9c). Infact, morphine binds Asp147, thus stabilizing itself in the orthosteric binding site. Compound **5** shows an undulatory movement, justified by its interaction not only with Asp216 on

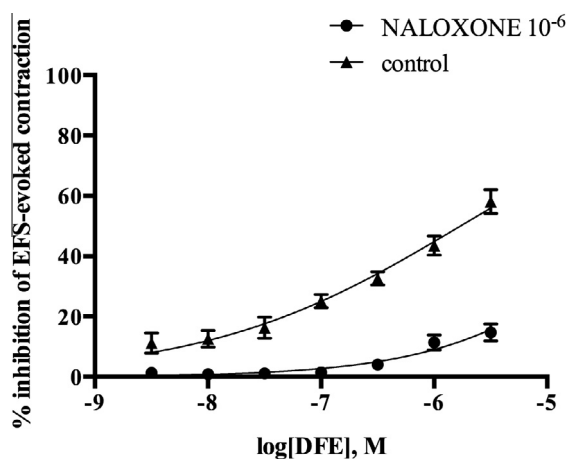


Figure 5. Effects of DFE in the electrically stimulated guinea pig ileum in the absence and presence of naloxone (10^{-6} M). Data represent means \pm SEM of 6–8 separate experiments.

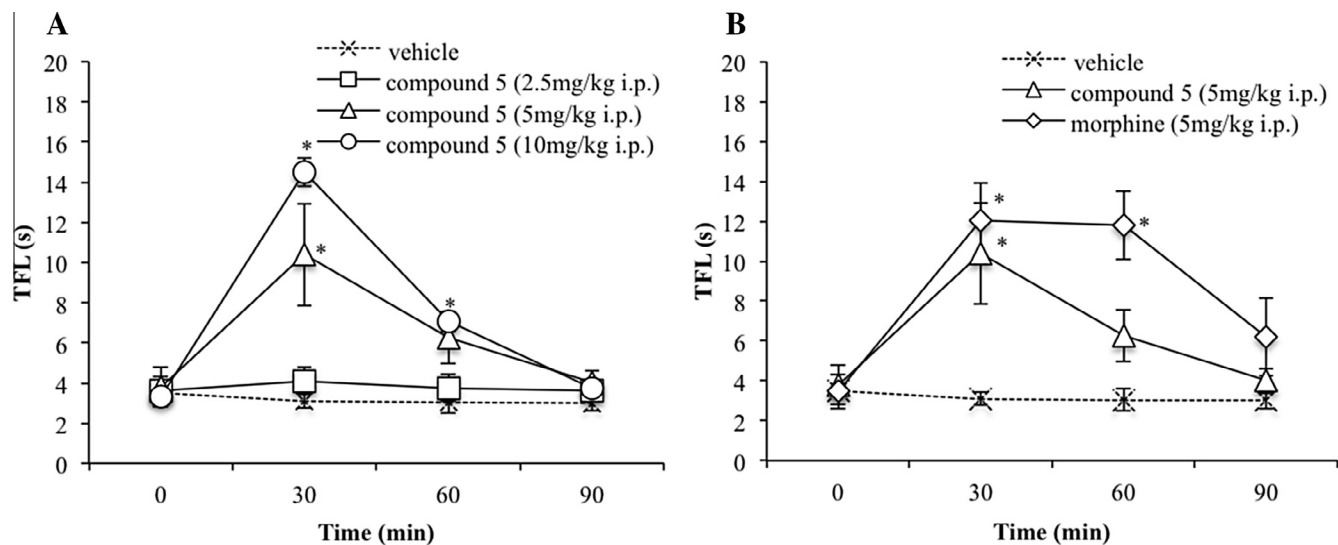


Figure 6. Antinociceptive effect of different doses of compound **5** Panel A. Comparison between analgesic effect of morphine (5 mg/kg ip) and **5** (5 mg/kg ip) Panel B. Data are expressed as the mean \pm SD. * p <0.05 versus saline-treated rats ($n = 8$); # p <0.05 versus saline-treated rats ($n = 8$).

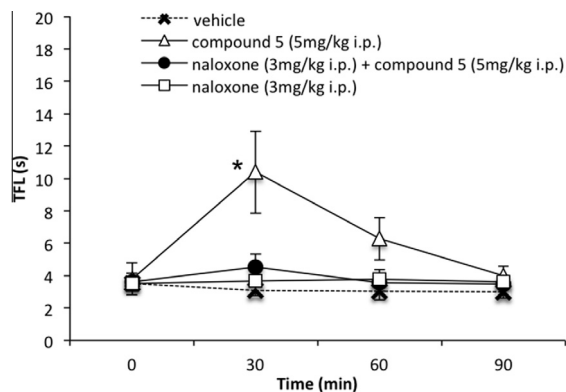


Figure 7. Effect of naloxone (3 mg/kg ip) on **5** analgesia. Data are expressed as the mean \pm SD. * p <0.05 versus saline-treated rats ($n = 8$); ** p <0.05 versus **5**-treated rats ($n = 8$).

ECL2 by the protonated nitrogen moiety on benzomorphan nucleus, (Fig. 12) but also with cysteines 140 and 217 with which interacts with the phenolic group. More interesting, compound **5**,

also presents an arene-arene stabilization between its diphenylic fragment and Tyr326 on TM7 (Fig. 10). Noteworthy, compound **5** interacts with its diphenylic portion with His297, proposed as relevant residue in the site directed mutagenesis studies conducted on MOR by Bot et al. in 1997.⁵¹

DAMGO shows an unstable evolution up to 10 ns. During this period of time it interacts by its tyrosine fragment with Asp147. After 10 ns, it appears to reach a stabilization by posing close to Ile144 and the aforementioned cysteines with its tyrosine group, to Trp318 with its phenolic portion and to Tyr75 with an H-arene interaction.

Altogether the above consideration allow us to hypothesize that compound **5** might not be sensitive to Naloxone antagonism because of the strong interaction with ECL2 amino acids and tyrosine residues. This interaction might be responsible of a slow dissociation rate from receptor as observed by Virk et al. for buprenorphine.³⁴

To evaluate possible evidence of different pathways for MOR activation, the change in the distance between Asp147 and Tyr326 was carefully examined and compared with that observed for the free protein. As reported in Figure S5, a stable reduction of about 2 Å is observed for compound **5** and DAMGO.

To better understand the role of the benzomorphan pharmacophoric group of **5**, we compared the poses in the LBD of LP1, whose molecular dynamic studies were recently published.¹⁴ LP1, displaced by Naloxone despite the pharmacophoric similarities with **5**, shows remarkable diversities in the docking poses within the MOR. First of all, the shorter amminic spacer and the presence of only one benzene ring makes it able to directly bind the receptor on ECL2 with its amidic group, thus greatly reducing its LBD occupancy. Probably for this reason, LP1 is able to have also a good interaction with DOR, whose LBD is smaller than that of MOR. LP1 shows an unstable interaction between its phenolic group and Asp147, for a few ns (Fig. 8). However, a non classical interaction seems to be imposed by the benzomorphan moiety with cysteines 140 and 217 in the LBD. LP1 shows a disposition similar to that of **5** in the interaction of Asp216 with the benzomorphan protonated amino group and of the above mentioned cysteines with the phenolic portion (Figs. S3b and S4a).

Trying to understand the pharmacological role of this 'allosteric' site with respect to the 'orthosteric' of morphine, we thought to evaluate, in our system, the dynamic characteristics of TRV-130,

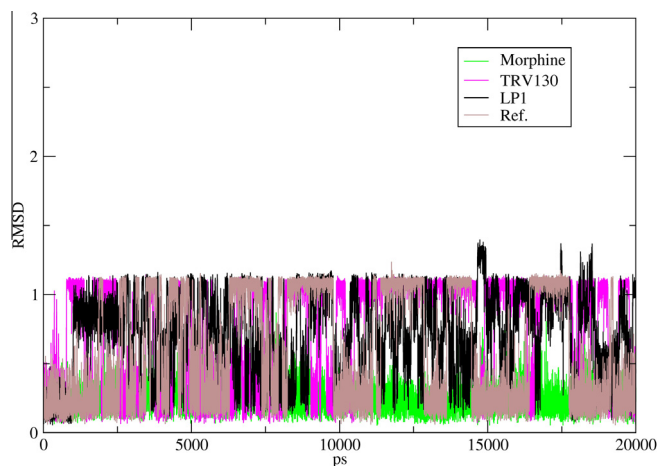


Figure 8. RMSD of Asp147 in presence of morphine, LP1 and TRV130 and free protein. Simulation times are expressed in ps.

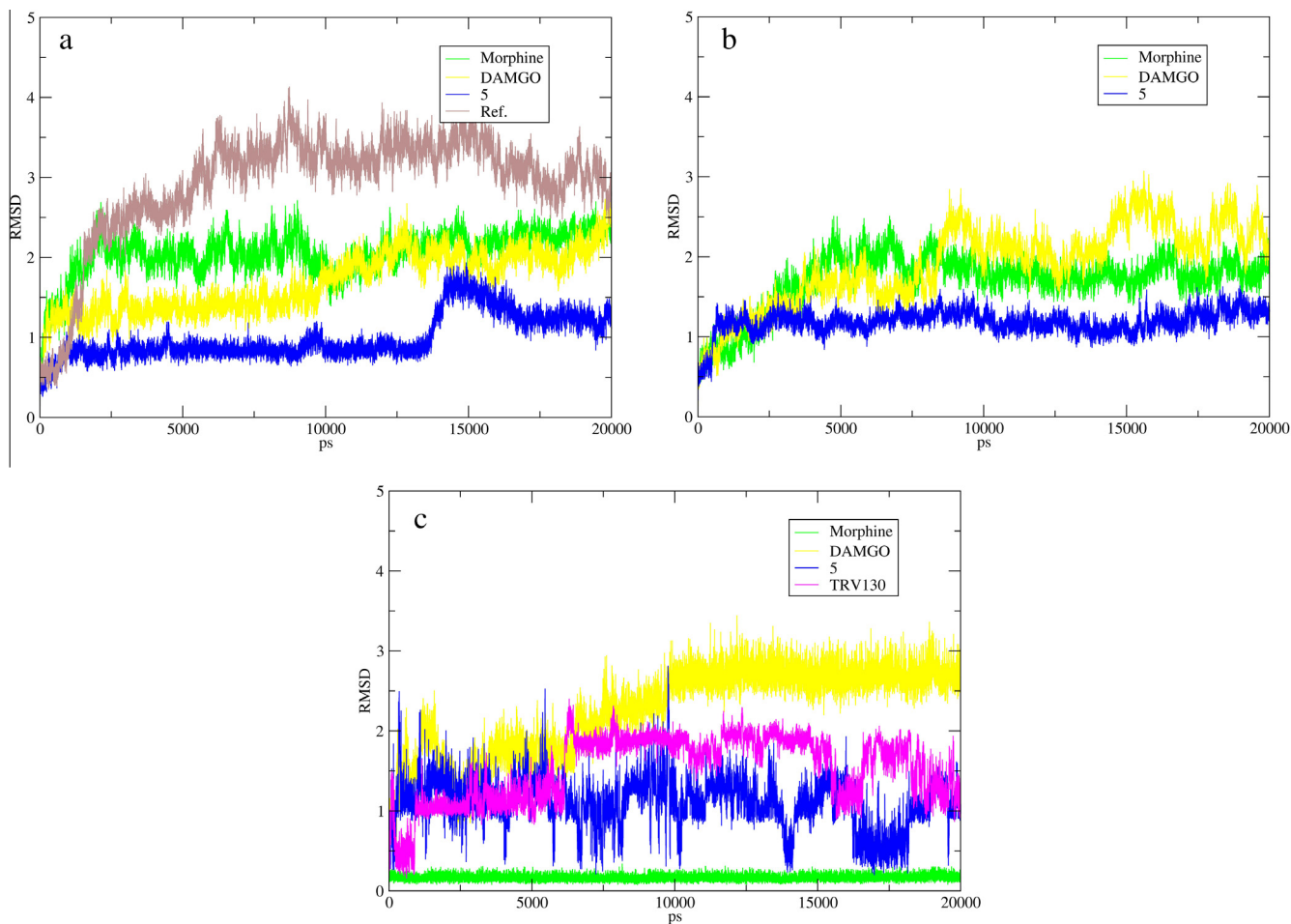


Figure 9. (a) RMSD of TM4 in presence of morphine, DAMGO, compound **5** and without ligand (b) RMSD of TM6 in presence of morphine, DAMGO and compound **5** (c) RMSD of heavy atoms of morphine, DAMGO, compound **5** and TRV130. Simulation times are expressed in ps.

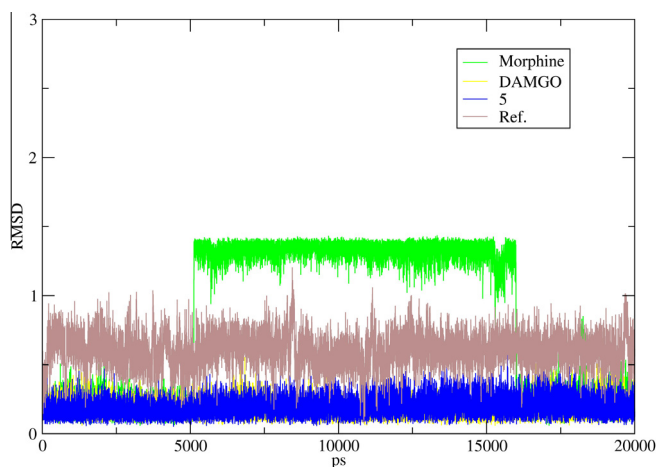


Figure 10. RMSD of Tyr326 in presence of morphine, DAMGO, compound **5**. Simulation times are expressed in ps.

a recently synthesized MOR agonist, able to activate β -arrestins circuit with a limited activation of the G-protein mediated pathway.¹⁴ TRV-130 results clearly allocated in the region of the LBD close to the ECL2 (Fig. 11) for 7.5 ns. This behavior is confirmed by a hydrogen bonding interaction between Asp216 and the protonated nitrogen on 3-methoxy-tiophen-2-yl moiety (Fig. 12).

After 7.5 ns, TRV-130 moves with this fragment to a stable pose superimposable to that of the benzomorphan group of **5** (Fig. 13). The interaction of **5** with Asn127 and Tyr128 remains peculiar.⁴⁷

The ability of TRV-130, compared to morphine (and purportedly morphine-like compounds), to occupy a non-classical site could be the cause of a different activation of protein pathway (Fig. 14).

In Figures 13 and 15, it is possible to evaluate TRV-130 positional changes in comparison with **5**, in the LBD, before (magenta) and after (purple) 7.5 ns. Only after 7.5 ns an engagement of the Cys140 residue is observed for both compounds (Fig. 9c). It is noteworthy to observe that the RMSD of Thr208, which is located on ECL2 close to the 4th TM domain, shows an important difference between TRV-130 and compound **5** (Fig. 13). As observed in Figure 15, a strong change is observed only for **5** after 7.5 ns, thus allowing to hypothesize a possible relevant role of Thr208 in the MOR allosteric LBD, as a consequence of ECL2 conformational changes after activation. Placement differences of TRV-130 and **5** with respect to the ECL2 are a possible justification of naloxone failure in antagonizing compound **5** but not TRV-130.

In conclusion, **5** seems to establish a fundamental hydrogen bonding interaction with Asp216 in ECL2. Compound **5** also possesses a critical arene–arene interactions with Tyr326 and Tyr128 with a benzomorphan phenol ring, and also strongly binds cysteines 217 and 140, which are involved in the disulfur bridge. This perturbation, relevant to provoke receptor conformational changes, was also observed with TRV-130 (Fig. S3a). Similarly to morphine, LP1 and DAMGO showed no changes (Figs. 3b, S4a–b).

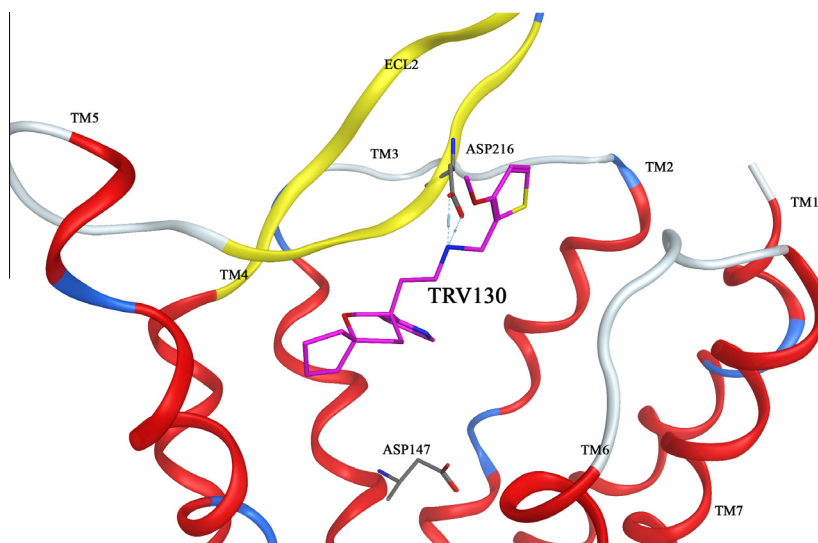


Figure 11. Pose of TRV130 in the binding pocket of mu opioid receptor and its interaction with Asp216 on ECL2 (figure captured at 2 ns).

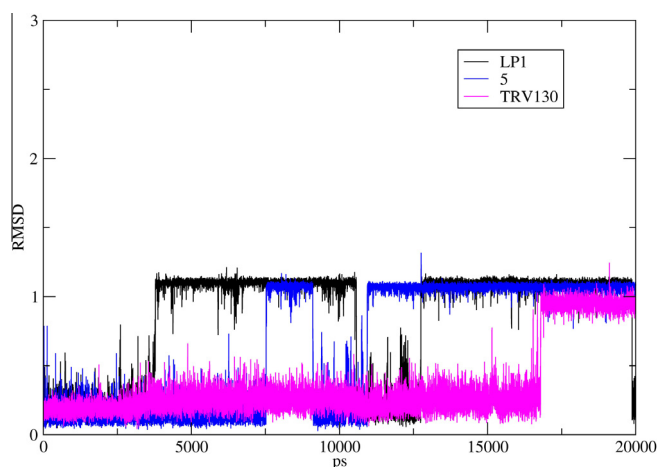


Figure 12. RMSD of Asp216 in presence of LP1, TRV130 and compound 5. Simulation times are expressed in ps.

3. Conclusions

In this study, the synthesis of 6,7-benzomorphanic derivatives, analogues of LP1 and bearing a diphenylic fragment and the peculiar pharmacological properties of compound **5** were reported. Specifically, compound **5** was a selective high affinity MOR agonist with in vivo antinociceptive activity. In the GPI, it was able to block electric stimulation not reversed by Naloxone. Molecular dynamic studies were conducted on compound **5** and on various established MOR agonists, in order to detect possible analogies and differences in their interactions with the amino acid residues present in the MOR LBD. Morphine, LP1, DAMGO and TRV130 were selected for the study.

As is widely known from mutagenesis data, we confirmed the interaction of morphine with Asp147, considered critical for high agonist binding affinity and full inhibition of cAMP.⁵² Interactions with Asn127 and Ile 144 were also observed.

In line with what has been recently observed for the δ peptides, and considered possible also for the μ , by Fenalti et al.,⁵⁴ in our experiments, DAMGO, initially interacts with Asp147 with a high

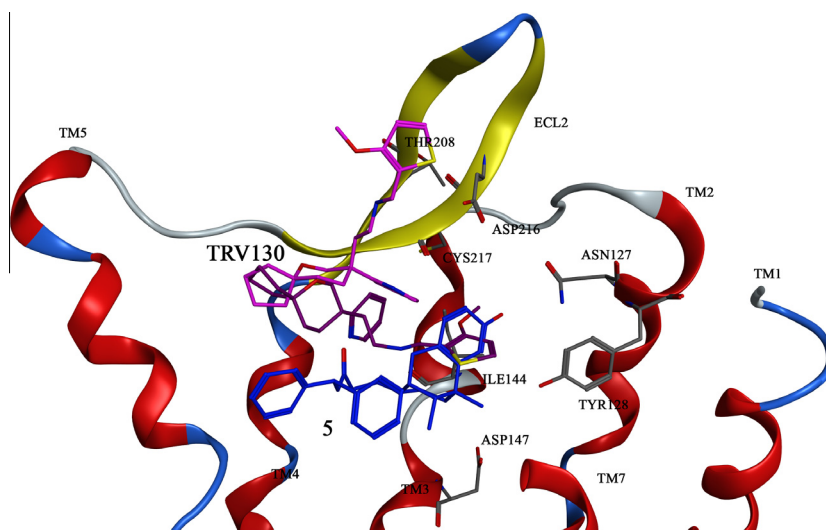


Figure 13. Two poses of TRV-130, at 2 ns (magenta) and at 8 ns (purple), showing a movement of about 7.6 Å. In blue compound **5** captured at 5 ns.

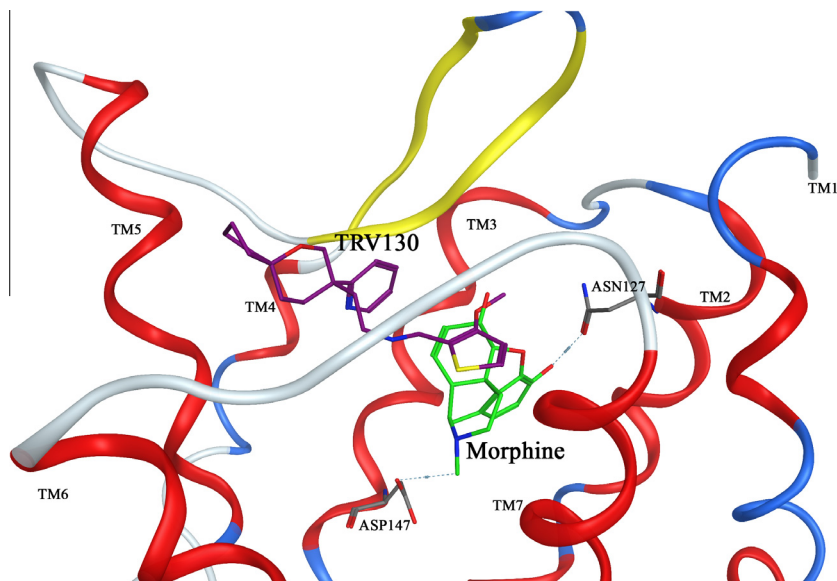


Figure 14. TRV130 (purple) and morphine (green) with respect to Asp147, captured at 8 ns.

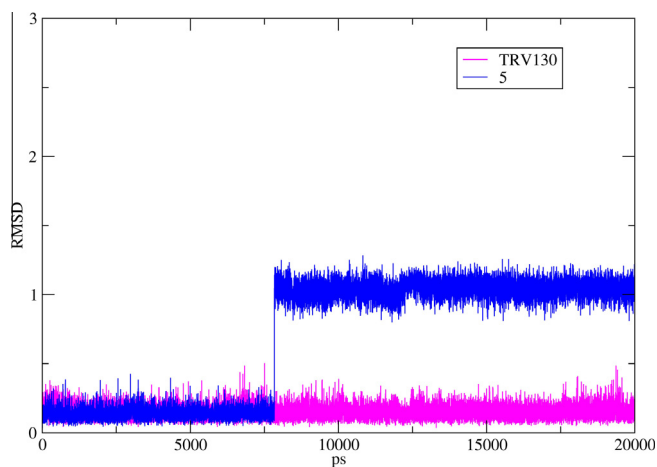


Figure 15. Involvement of TRV130 and compound **5** on RMSD of Thr208. Simulation times are expressed in ps.

occupancy value displayed for 3 ns (data not showed) and then stabilizes itself in an allosteric binding pocket interacting with Cys217 and Cys140 of the disulfide bridge. Interestingly, DAMGO, in its final pose, superimposes compound **5**, which binding site was defined by the a stable interaction with the following residues: Asn127(TM2), Tyr128(TM2), Asp216(ECL2), Tyr148(TM3), Tyr299(TM6) and Tyr326(TM7).

Dynamic studies conducted on TRV-130 showed that, similarly to compound **5**, it interacts with the above mentioned cysteines and ECL2, but less strongly than **5** coherently with the different behavior observed toward naloxone antagonism. LP1, the prototypic benzomorphan derivative acting as MOR agonist/DOR antagonist, interacts, as recently reported,⁴⁶ with the above mentioned cysteines, but neither does interact with Asp147 nor shows the ability to form a stable arene–arene interaction with the tyrosines on 6th and 7th TM domain.

If we assume that morphine activates the G-protein pathway and the β -arrestin2 circuit alone with its orthosteric occupancy in the LBD and that TRV-130 is able to activate the G-protein pathway and both the β -arrestin1 and 2 circuits without any interaction with Asp147 but occupying the allosteric LBD, we can

assume that DAMGO might play a double role in the biochemical signaling of MOR.⁵³

The present dynamic simulation also indicates that ECL2, with its disulfide bridge, may play an important role on MOR conformational stabilization. ECL2 seems to be involved in the maintenance of ligands in the LBD. Possibly, the lack of the ligand initial interaction with the tyrosines plays a role in naloxone capability to displace agonists.

In conclusion, these studies seem to suggest the possibility that complete MOR signaling can be obtained by occupying sites in the MOR LBD other than those occupied by morphine and its analogues. Further biochemical and pharmacological studies with allosteric ligands are necessary to investigate antinociceptive pathways and to have information on signal transduction and on the processes of receptor activation/deactivation.

4. Experimental

4.1. Chemistry

4.1.1. General procedure (A) for the preparation of 3-bromo-*N*-substituted- and 3-bromo-*N,N*-disubstituted propanamide derivatives (**1–3**)

To a solution of bromoacetyl chloride (1.40 g, 8.17 mmol) in 10 mL of dry THF cooled at 0 °C, under argon atmosphere, was added dropwise, under vigorous stirring, a solution of the appropriate amine (5.45 mmol) and triethylamine (0.276 g, 2.72 mmol) in dry THF (10 mL). After 30 min at 0 °C and 30 min at room temperature the reaction mixture was quenched by the addition of 50 ml of H₂O and extracted with dichloromethane (3 × 50 ml). The combined organic extracts were washed with saturated NaHCO₃ and brine, and then dried over anhydrous Na₂SO₄. Evaporation under reduced pressure gave the crude 3-bromopropanamide derivatives (**1–3**) which were purified by flash chromatography on silica gel, using CH₂Cl₂ and cyclohexane as eluent.

4.1.1.1. 3-Bromo-*N*-(2,2-diphenylethyl)propanamide (1**).** White solid (93%). mp: 98–100 °C. ¹H NMR (CDCl₃) δ ppm: 7.28–7.35 (m, 4H); 7.20–7.27 (m, 6H); 5.55 (br s, 1H); 4.20 (t, *J* = 8.0 Hz, 1H); 3.92 (dd, *J* = 8.0, 6.0 Hz, 2H); 3.55 (t, *J* = 6.50 Hz, 2H); 2.61 (t, *J* = 6.50 Hz, 2H). Anal. Calcd for C₁₇H₁₈BrNO: C, 61.46; H, 5.46; N, 4.22. Found: C, 61.51; H, 5.51; N, 4.29.

4.1.1.2. 3-Bromo-N-(diphenylmethyl)-N-methylpropanamide (2). White solid (73%). mp: 102–104 °C. ¹H NMR (CDCl₃) δ ppm: 7.13–7.41 (m, 10H); 6.27 (s, 1H); 3.72 (s, *J* = 7.00 Hz, 2H); 3.03 (t, *J* = 7.00 Hz, 2H); 2.82 (s, 3H). Anal. Calcd for C₁₇H₁₈BrNO: C, 61.46; H, 5.46; N, 4.22. Found: C, 61.59; H, 5.53; N, 4.23.

4.1.1.3. 3-Bromo-N-(diphenylmethyl)propanamide (3). White solid (74%). mp: 96–98 °C. ¹H NMR (CDCl₃) δ ppm: 7.19–7.37 (m, 10H); 6.25 (s, 1H); 3.64 (t, *J* = 6.60 Hz, 2H); 2.81 (t, *J* = 6.6 Hz, 2H). Anal. Calcd for C₁₆H₁₆BrNO: C, 60.39; H, 5.07; N, 4.40. Found: C, 60.45; H, 5.06; N, 4.53.

4.1.1.4. 3-Bromo-1-(1-phenyl-1,2,3,4-tetrahydronaphthalen-2-yl)propan-1-one (4). White solid (71%). mp: 110–112 °C. ¹H NMR (CDCl₃) ppm: 7.04–7.37 (m, 10H); 6.93 (s, 1H); 3.64–3.81 (m, 3H); 3.40–3.59 (m, 1H); 2.75–3.19 (m, 4H). Anal. Calcd for C₁₈H₁₈BrNO: C, 62.80; H, 5.27; N, 4.07. Found: C, 62.88; H, 5.29; N, 4.13.

4.1.1.5. General procedure (B) for the preparation of N-substituted cis-(–)-N-normetazocine derivatives (5–7). A mixture of cis-(–)-(1R,5R,9R)-N-normetazocine (150.00 mg, 0.69 mmol), the appropriate 3-bromoamide derivatives (**1–3**, 1.04 mmol), NaHCO₃ (87.37 mg, 1.04 mmol) and a catalytic amount of KI was stirred in dry methanol (10 mL) at 50 °C for 24 h under an argon atmosphere in the dark. The reaction mixture was filtered and the solid residue was rinsed with methanol. Concentration under reduced pressure of the combined filtrate and washing methanol solutions gave a solid/semisolid residue which was purified by flash chromatography on silica gel using as eluent CH₂Cl₂/MeOH (95:5, v/v). Immediately before the purification process the crude product was treated with an appropriate amount of eluent, filtered and loaded in the column for the chromatographic separation.

4.1.2. N-(2,2-Diphenylethyl)-3-[(2R,6R,11R)-8-hydroxy-6,11-dimethyl-1,4,5,6-tetrahydro-2,6-methano-3-benzazocin-3(2H)-yl]propanamide (5)

Yellowish solid (65%); mp: 156–158 °C; –49° (c 1.0, MeOH); ¹H NMR (CDCl₃) δ ppm: 8.83 (br s, 1H); 7.33–7.17 (m, 10H); 6.86–6.81 (m, 1H); 6.65–6.61 (m, 1H); 6.69–6.73 (m, 1H); 4.22 (t, *J* = 8 Hz, 1H); 3.97–3.80 (m, 2H); 2.73–2.50 (m, 5H); 2.41–2.20 (m, 3H); 1.95–1.84 (m, 1H); 1.37–1.14 (m, 3H); 1.23 (s, 3H); 0.72 (d, *J* = 7 Hz, 3H). Anal. Calcd for C₃₁H₃₆N₂O₂: C, 79.45; H, 7.74; N, 5.98. Found: C, 79.71; H, 7.79; N, 6.01.

4.1.2.1. N-(Diphenylmethyl)-3-[(2R,6R,11R)-8-hydroxy-6,11-dimethyl-1,4,5,6-tetrahydro-2,6-methano-3-benzazocin-3(2H)-yl]-N-methylpropanamide (6). Yellowish solid (42%); mp: 172–174 °C; –52° (c 1.0, MeOH); ¹H NMR (CDCl₃) δ ppm: 7.41–7.11 (m, 10H); 6.94–6.86 (m, 1H); 6.80–6.76 (m, 1H); 6.75–6.70 (m, 1H); 6.46–6.41 (m, 1H); 2.68–2.41 (m, 5H); 2.40–2.20 (m, 3H); 2.07–1.99 (m, 1H); 1.21–1.46 (m, 3H); 1.34 (s, 3H); 0.85 (d, *J* = 6.5 Hz, 3H). Anal. Calcd for C₃₁H₃₆N₂O₂: C, 79.45; H, 7.74; N, 6.83. Found: C, 80.15; H, 7.78; N, 6.03.

4.1.2.2. N-(Diphenylmethyl)-3-[(2R,6R,11R)-8-hydroxy-6,11-dimethyl-1,4,5,6-tetrahydro-2,6-methano-3-benzazocin-3(2H)-yl]propanamide (7). Yellowish solid (48%); mp: 168–170 °C; –58° (c 1.0, MeOH); ¹H NMR (CDCl₃) δ ppm: 9.98 (br s, 1H); 7.38–7.20 (m, 10H); 6.89–6.84 (m, 1H); 6.68–6.54 (m, 2H); 6.25–6.20 (m, 1H); 2.89–2.70 (m, 4H); 2.67–2.32 (m, 4H); 2.05–1.97 (m, 1H); 1.18–1.44 (m, 3H); 1.23 (s, 3H); 0.67 (d, *J* = 7 Hz, 3H). Anal. Calcd for C₃₀H₃₄N₂O₂: C, 79.26; H, 7.54; N, 6.16. Found: C, 79.58; H, 7.55; N, 6.19.

4.1.2.3. 3-[4-Hydroxy-1,13-dimethyl-10-azatricyclo[7.3.1.0^{2,7}]trideca-2,4,6-trien-10-yl]-1-(1-phenyl-1,2,3,4-tetrahydronaphthalen-2-yl)propan-1-one (8±). Yellowish solid (84%); mp:

154–156 °C; ¹H NMR (CDCl₃) δ ppm: 7.26 (m, 3H); 7.23 (m, 3H); 7.19 (m, 2H); 7.08 (m, 1H); 6.98 (m, 1H); 6.66 (m, 1H); 6.1 (s, 0.4H); 5.30 (s, 0.6H); 3.85 (m, 1H); 3.53 (m, 1H); 3.46 (m, 1H); 3.17 (m, 2H); 2.99 (m, 4H); 2.81 (m, 5H); 2.76 (m, 2H); 2.19 (m, 2H); 2.15 (d, 2H); 2.01 (s, 1H); 1.31 (s, 3H); 0.81 (d, 3H). Anal. Calcd for C₃₂H₃₈N₂O₂: C, 79.63; H, 7.93; N, 5.80. Found: C, 79.58; H, 8.02; N, 5.73.

HPLC separations were performed on a Perkin Elmer Flexar FX-10 UHPLC System equipped with a single-wavelength UV-visible detector (Perkin Elmer, Italy). Separations were performed on Chiralpak AD-H analytical column (250 mm × 4.6 mm, 5 μ particle size, Chiral Technology Europe, Illkirch Cedex France). The mobile phase consisted of hexane/2-propanol (90:10 v/v) at flow rate of 0.5 ml/min. The wavelength was set at 254 nm and the column was maintained at 23 °C.

4.1.2.4. 3-[(1R,13R)-4-Hydroxy-1,13-dimethyl-10-azatricyclo[7.3.1.0^{2,7}]trideca-2,4,6-trien-10-yl]-1-(1R)-1-phenyl-1,2,3,4-tetrahydronaphthalen-2-yl]propan-1-one (8a). Yellowish solid (63%); mp: 152–154 °C; [α]_D²⁰: –50° (c 1.0, MeOH); ¹H NMR (CDCl₃) δ ppm: 7.26 (m, 3H); 7.23 (m, 3H); 7.19 (m, 2H); 7.08 (m, 1H); 6.98 (m, 1H); 6.66 (m, 1H); 6.1 (s, 0.4H); 5.30 (s, 0.6H); 3.85 (m, 1H); 3.53 (m, 1H); 3.46 (m, 1H); 3.17 (m, 2H); 2.99 (m, 4H); 2.81 (m, 5H); 2.76 (m, 2H); 2.19 (m, 2H); 2.15 (d, 2H); 2.01 (s, 1H); 1.31 (s, 3H); 0.81 (d, 3H). Anal. Calcd for C₃₂H₃₈N₂O₂: C, 79.63; H, 7.93; N, 5.80. Found: C, 79.60; H, 8.00; N, 5.69.

4.1.2.5. 3-[(1R,13R)-4-hydroxy-1,13-dimethyl-10-azatricyclo[7.3.1.0^{2,7}]trideca-2,4,6-trien-10-yl]-1-(1S)-1-phenyl-1,2,3,4-tetrahydronaphthalen-2-yl]propan-1-one (8b). Yellowish solid (52%); mp: 150–152 °C; [α]_D²⁰: 52° (c 1.0, MeOH); ¹H NMR (CDCl₃) δ ppm: 7.26 (m, 3H); 7.23 (m, 3H); 7.19 (m, 2H); 7.08 (m, 1H); 6.98 (m, 1H); 6.66 (m, 1H); 6.1 (s, 0.4H); 5.35 (s, 0.6H); 3.85 (m, 1H); 3.53 (m, 1H); 3.46 (m, 1H); 3.17 (m, 2H); 2.99 (m, 4H); 2.81 (m, 5H); 2.76 (m, 2H); 2.19 (m, 2H); 2.15 (d, 2H); 2.01 (s, 1H); 1.25 (s, 3H); 0.75 (d, 3H). Anal. Calcd for C₃₂H₃₈N₂O₂: C, 79.63; H, 7.93; N, 5.80. Found: C, 80.02; H, 7.88; N, 5.88.

4.2. In vitro radioligand binding assay

MOR, KOR and DOR affinities were investigated by CEREP in 500 competition experiments with radioligands. In the Mor assay, the selective agonist ligand DAMGO was used as radioligand. To label Kor receptors was employed U 50488 as agonist radioligand. For Dor was used DPDPE as radioligand.

In Mor assay, HEK-293 cells were used as a source of receptors. For Kor assay rat CHO cells and for Dor human CHO cells were used. Non-specific binding was determined in the presence of nal-trexone (10 μM). Eight concentrations of each compound (0.3–1000 nM) were used in the assays.

4.3. In ex vivo pharmacology

4.3.1. Guinea-pig ileum preparation

Sections of guinea-pig ileum longitudinal muscle/myenteric plexus were prepared according to Kinney et al. (1995) with minor modifications. Male Dunkin–Hartley guinea-pigs (200–300 g) (Harlan Laboratories, S.Pietro al Natisone (UD) were killed by decapitation. The intestines were exteriorized, the ileo-caecal junction located and 5 cm of the terminal ileum discarded. Approximately 30 cm of the terminal ileum was removed and the lumen flushed with Krebs solution (in mM: 118 NaCl, 4.75 KCl, 2.45 CaCl₂, 1.71 MgCl₂, 25.0 NaHCO₃, 0.93 KH₂PO₄, 11 glucose). Four 2 cm long segments of the ileum were secured on to a perspex holder supporting two parallel platinum wire electrodes and placed in a

20 ml isolated organ bath containing Krebs solution at 37.0 °C and bubbled with 5% CO₂/95% O₂. The strips were placed under a 2 g load and contractility measured using an appropriate transducer connected to a PowerLab 4/20 recorder (ADInstruments, Castle Hill, NSW, Australia). After 60 min equilibration, maximal contractions of the tissue were elicited by transmural stimulation using single pulses (0.1 Hz, 0.3 ms, 200 mA) delivered by a Digitimer multisystem D330 stimulator.

Following a 60–90 min equilibrium period, during which the Krebs solution was changed several times, test compounds were added cumulatively, allowing a minimum of 5 min before additional compound was added to the bath.

4.3.2. Data analysis

Electrically-evoked contractions have been expressed as a percentage of the contraction. The effectiveness of a given compound to inhibit electrically induced contraction was measured as the percentage change from baseline. The concentration of a given test compound eliciting half-maximal inhibition of the electrically induced contraction (EC₅₀) was determined by non-linear curve fitting (Prism v. 3.0, GraphPad) using the mean response of at least three separate trials as the given response for a single concentration. The potency of the opioid receptor agonists in the absence and presence of the antagonists was assessed as the negative logarithm of the concentration required to cause 50% of the maximum response (pD₂).

4.4. In vivo pharmacology

4.4.1. Animals

Male Swiss CB1 mice (Harlan Laboratories, S.Pietro al Tisonese (UD)) weighing 25–30 g were housed six to a cage. Animals were kept at a constant room temperature (25 ± 1 °C) under a 12:12 h light and dark cycle with free access to food and water. Each mouse was used for only one experiment. Experimental procedures were approved by the Local Ethical Committee (IACUC) and conducted in accordance with international guidelines as well as European Communities Council Directive and National Regulations (CEE Council 86/609 and DL 116/92).

4.4.2. Tail-Flick Test

Nociception was evaluated by the radiant heat tail-flick test. Briefly, it consisted of irradiation of the lower third of the tail with an infrared source (Ugo Basile, Comerio, Italy). The day before the experiment, mice were habituated to the procedure for measuring nociception threshold. Experiments were performed at room temperature (25 ± 1 °C). The basal pre-drug latency was established between 3 and 4 s and was calculated as the average of the first three measurements, which were performed at 5 min intervals. A cutoff latency of 10 s was established to minimize damage to the tail. Post-treatment tail flick latencies (TFLs) were determined at 30, 60 and 90 min after intraperitoneal (ip) injection.

4.4.3. Statistical Analysis

Data are expressed as mean values (SEM analysis of variance (ANOVA) followed by the post hoc 'Student–Newman–Keuls' test were performed to assess significance using the Instat 3.0 software (GraphPad Software, San Diego, CA). *P* < 0.05 was considered significant.

4.4.4. Docking and Molecular Dynamics Methods

Files containing MOR atomic spatial coordinates were downloaded from ProteinDataBank (4DKL 2.8 Å and 5C1M 2.1 Å). They were carefully checked for defects, i.e. ECL3 loop absence (between the third and the fourth transmembrane domains) in 4DKL model. Errors, T4L and Nb39 were corrected or eliminated by MOE soft-

ware (developed by Chemical Computing Group).⁴⁸ The obtained proteins have undergone relaxing dynamic cycles for 20 ns by NAMD software in NVT and NPT ensemble (*T* = 300°K; *P* = 1.01325 bar). The same conditions were applied to all other simulations. Receptors were then inserted in a phospholipidic bilayer, made by 260 dipalmitoylphosphatidylcholine (POPC) residues, and a water bilayer (11485 water molecules) was created (grid dimension: 113 × 112 × 79 Å). Both procedures were effectuated by charmm-gui.org (default settings), a web-based graphical user interface able to generate various molecular systems.⁴⁹ Additional relaxing cycles were further accomplished for other 20 ns. Checked the stability of the systems, docking studies were conducted by MOE with a 'Triangle Matcher' placement methodology. Ligands were minimized with FFM94X forcefield (developed for the MOE software) with lowest minimization gradient. Charges were calculated by LigX, MOE subprogram. Conformational studies were then performed, using systematic and stochastic methods. Databases were created with more than 15,000 conformations. Rescoring on databases was then effectuated (London dG and GBVI/WSA dG). After evaluation of docking scores and interaction ligand energies, starting poses were chosen. During protein-membrane relaxing phases and docking evaluations, only one angstrom of RMSD gap through modified 4DKL and 5C1M was observed. The first was however selected to accomplish our studies. Subsequently, initial steps to run molecular dynamic studies were carried out. NAMD software⁵⁰ was chosen to conduct these studies and input files were prepared by tLeap developed in Amber12 and AmberTools 12 with 'ff12SB' and 'ff99SBildn' forcefield for protein and 'gaff' forcefield for ligands.⁴⁴ AmberTools 14 was utilized for membrane forcefield, in particular 'lipid11' and 'lipid14'. Ligand charges were obtained by Gaussian09. tLeap was used to neutralize complex charge. In an initial phase, protein and ligand are fixed to obtain a good merge between ligand–protein system and phospholipidic bilayer. After this initial step, all components were slowly released (backbone and ligand in a first phase and later α-carbon). POPC is always completely free. Every final production cycle was conducted 10 times and the mean was utilized to create a RMSD curves (see in the text). Measurements up to 50 ns not showed relevant variations.

Acknowledgments

This work was supported by a FP6 European Grant 'Normolife' (LSHC-CT-2006-037733) and by 'Finanziamento della Ricerca' FIR2014 granted by University of Catania. The authors gratefully acknowledge Fabbrica Italiana Sintetici (Italy) for providing (±)-*cis*-*N*-normetazocine.

A. Supplementary data

Supplementary data associated with this article can be found, in the online version, at <http://dx.doi.org/10.1016/j.bmc.2016.08.057>.

References and notes

- Melnikova, I. *Nat. Rev. Drug Disc.* **2010**, *9*, 589.
- Power, I. *Br. J. Anaesth.* **2011**, *107*, 19.
- Gherlandini, C.; Di Cesare Mannelli, L.; Bianchi, E. *Clin. Cases Miner. Bone Metab.* **2015**, *12*, 219.
- Waldhoer, M.; Bartlett, S. E.; Whistler, J. L. *Annu. Rev. Biochem.* **2004**, *73*, 953.
- Cox, B. M.; Goldstein, A.; Hi, C. H. *Proc. Natl. Acad. Sci. U.S.A.* **1976**, *73*, 1821.
- Zadina, J. E.; Hackler, L.; Ge, L. J.; Kastin, A. J. *Nature* **1997**, *386*, 499.
- Benyamin, R.; Trescot, A. M.; Datta, S.; Buenaventura, R.; Adlaka, R.; Sehgal, N.; Glaser, S. E.; Vallejo, R. *Pain Physician* **2008**, *11*, S105.
- Contet, C.; Kieffer, B. L.; Befort, K. *Curr. Opin. Neurobiol.* **2004**, *14*, 370.
- Gaveriaux-Ruff, C.; Kieffer, B. L. *Neuropeptides* **2002**, *36*, 62.
- Casy, A. F.; Parfitt, R. T. *Opioid Analgesics: Chemistry and Receptors*; Plenum Press: New York, 1986.
- Trafton, J. A.; Ramani, A. *Curr. Pain Headache Rep.* **2009**, *13*, 24.

12. Grond, S.; Sablotzki, A. *Clin. Pharmacokinet.* **2004**, *43*, 879–208.
13. Kenakin, T. J. *Pharmacol. Exp. Ther.* **2011**, *336*, 296.
14. DeWire, S. M.; Yamashita, D. S.; Rominger, D. H.; Liu, G.; Cowan, C. L.; Graczyk, T. M.; Chen, X. T.; Pitis, P. M.; Gotchev, D.; Yuan, C.; Koblisch, M.; Lark, M. W.; Violin, J. D. *J. Pharmacol. Exp. Ther.* **2013**, *344*, 708.
15. Martin, M.; Matifas, A.; Maldonado, R.; Kieffer, B. L. *Eur. J. Neurosci.* **2003**, *17*, 701.
16. Matthes, H. W.; Maldonado, R.; Simonin, F.; Valverde, O.; Slowe, S.; Kitchen, I.; Befort, K.; Dierich, A.; Le Meur, M.; Dollé, P.; Tzavara, E.; Hanoune, J.; Roques, B. P.; Kieffer, B. L. *Nature* **1996**, *383*, 819.
17. Hanauer, S. B. *Rev. Gastroenterol. Disord.* **2008**, *8*, 15.
18. Portoghese, P. S. *J. Med. Chem.* **1965**, *8*, 609.
19. Dietis, N.; Rowbotham, D. J.; Lambert, D. G. *Br. J. Anaesth.* **2011**, *107*, 8.
20. Andoh, T.; Tageta, Y.; Konno, M.; Yamaguchi-Minamoto, T.; Takahata, H.; Nojima, H.; Kuraishi, Y. *J. Pharmacol. Sci.* **2008**, *106*, 667.
21. Law, P. Y.; Reggio, P. H.; Loh, H. H. *Trends Biochem. Sci.* **2013**, *38*, 275.
22. Loh, H. H.; Liu, H. C.; Cavalli, A.; Yang, W.; Chen, Y. F.; Wei, L. N. *Brain Res. Mol. Brain Res.* **1998**, *54*, 321–320.
23. Sora, I.; Takahashi, N.; Funada, M.; Ujike, H.; Revay, R. S.; Donovan, D. M.; Miner, L. L.; Uhl, G. R. *Proc. Natl. Acad. Sci. U.S.A.* **1997**, *94*, 1544.
24. Al-Hasani, R.; Bruchas, M. R. *Anesthesiology* **2011**, *115*, 1363.
25. Gomes, I.; Jordan, B. A.; Gupta, A.; Trapaidze, N.; Nagy, V.; Devi, L. A. *J. Neurosci.* **2000**, *20*, RC110.
26. Gomes, I.; Filipovska, J.; Devi, L. A. *Methods Mol. Med.* **2003**, *84*, 157.
27. Gomes, I.; Gupta, A.; Filipovska, J.; Szeto, H. H.; Pintar, J. E.; Devi, L. A. *Proc. Natl. Acad. Sci. U.S.A.* **2004**, *101*, 5135.
28. Parenti, C.; Turnaturi, R.; Aricò, G.; Marrazzo, A.; Prezzavento, O.; Ronsisvalle, S.; Scoto, G. M.; Ronsisvalle, G.; Pasquinucci, L. *Life Sci.* **2012**, *90*, 957.
29. Pasternak, G. W.; Pan, Y. X. *Neuron* **2011**, *69*, 6.
30. Pasquinucci, L.; Prezzavento, O.; Marrazzo, A.; Amata, E.; Ronsisvalle, S.; Georgoussi, Z.; Fourla, D. D.; Scoto, G. M.; Parenti, C.; Aricò, G.; Ronsisvalle, G. *Bioorg. Med. Chem.* **2010**, *18*, 4975.
31. Parenti, C.; Turnaturi, R.; Aricò, G.; Gramowski-Voss, A.; Schroeder, O. H.; Marrazzo, A.; Prezzavento, O.; Ronsisvalle, S.; Scoto, G. M.; Ronsisvalle, G.; Pasquinucci, L. *Neuropharmacology* **2013**, *71*, 70.
32. He, S. Q.; Zhang, Z. N.; Guan, J. S.; Liu, H. R.; Zhao, B.; Wang, H. B.; Li, Q.; Yang, H.; Luo, J.; Li, Z. Y.; Wang, Q.; Lu, Y. J.; Bao, L.; Zhang, X. *Neuron* **2011**, *69*, 120.
33. Harold Suh, H.; Tseng, Liang-Fu. *J. Pharmacol. Exp. Ther.* **1988**, *245*, 587.
34. Virk, M. S.; Arttamangkul, S.; Birdsong, W. T.; Williams, J. T. *J. Neurosci.* **2009**, *29*, 7341.
35. Gomes, I.; Ljzerman, A. P.; Ye, K.; Maillet, E. L.; Devi, L. A. *Mol. Pharmacol.* **2011**, *79*, 1044.
36. Granier, S.; Manglik, A.; Kruse, A. C.; Kobilka, T. S.; Thian, F. S.; Weis, W. I.; Kobilka, B. K. *Nature* **2012**, *485*, 400.
37. Dehave-Hudkins, D. L.; Cortes Burgos, L.; Cassel, J. A.; Daubert, J. D.; Dehaven, R. N.; Mansson, E.; Nagasaka, H.; Yu, G.; Yaksh, T. J. *Pharm. Exp. Ther.* **1999**, *289*, 494.
38. Shannon, H. E.; Lutz, E. A. *Neuropharmacology* **2002**, *42*, 253.
39. Brine, G. A.; Berrang, B.; Hayes, J. P.; Carroll, F. I. *J. Heterocycl. Chem.* **1990**, *27*, 2139.
40. Wu, H.; Wacker, D.; Mileni, M.; Katritch, V.; Han, G. W.; Vardy, E.; Liu, W.; Thompson, A. A.; Huang, X. P.; Carroll, F. I.; Mascarella, S. W.; Westkaemper, R. B.; Mosier, P. D.; Roth, B. L.; Cherezov, V.; Stevens, R. C. *Nature* **2012**, *485*, 327.
41. Huang, W.; Manglik, A.; Venkatakrishnan, A. J.; Laeremans, T.; Feinberg, E. N.; Sanborn, A. L.; Kato, H. E.; Livingston, K. E.; Thorsen, T. S.; Kling, R. C.; Granier, S.; Gmeiner, P.; Husbands, S. M.; Traynor, J. R.; Weis, W. I.; Steyaert, J.; Dror, R. O.; Kobilka, B. K. *Nature* **2015**, *524*, 315.
42. Birdsong, W. T.; Arttamangkul, S.; Bunzow, J. R.; Williams, J. T. *Mol. Pharmacol.* **2015**, *88*, 816.
43. Case, D. A.; Darden, T. A.; Cheatham, T. E., III; Simmerling, C. L.; Wang, J.; Duke, R. E.; Luo, R.; Walker, R. C.; Zhang, W.; Merz, K. M.; Roberts, B.; Hayik, S.; Roitberg, A.; Seabra, G.; Swails, J.; Götz, A. W.; Kolossváry, I.; Wong, K. F.; Paesani, F.; Vanicek, J.; Wolf, R. M.; Liu, J.; Wu, X.; Brozell, S. R.; Steinbrecher, T.; Gohlke, H.; Cai, Q.; Ye, X.; Wang, J.; Hsieh, M.-J.; Cui, G.; Roe, D. R.; Mathews, D. H.; Seetin, M. G.; Salomon-Ferrer, R.; Sagui, C.; Babin, V.; Luchko, T.; Gusarov, S.; Kovalenko, A.; Kollman, P. A. *AMBER 12*; University of California: San Francisco, 2012.
44. Manglik, A.; Kruse, A. C.; Kobilka, T. S.; Thian, F. S.; Mathiesen, J. M.; Sunahara, R. K.; Pardo, L.; Weis, W. I.; Kobilka, B. K.; Granier, S. *Nature* **2012**, *485*, 321.
45. Chen, Xiao-Tao; Pitis, Philip; Liu, Guodong; Yuan, Catherine; Gotchev, Dimitar; Cowan, Conrad L.; Rominger, David H.; Koblisch, Michael; DeWire, Scott M.; Crombie, Aimee L.; Violin, Jonathan D.; Yamashita, Dennis S. *J. Med. Chem.* **2013**, *56*, 8019.
46. Pasquinucci, L.; Turnaturi, R.; Aricò, G.; Parenti, C.; Pallaki, P.; Georgoussi, Z.; Ronsisvalle, S. *Bioorg. Med. Chem.* **2016**.
47. Gentilucci, L.; Tolomelli, A.; De Marco, R.; Artali, R. *Curr. Med. Chem.* **2012**, *19*, 1587.
48. Molecular Operating Environment (MOE), 2013.08; Chemical Computing Group Inc., 1010 Sherbooke St. West, Suite #910, Montreal, QC, Canada, H3A 2R7, 2016.
49. Jo, S.; Kim, T.; Iyer, V. G.; Im, W. J. *Comput. Chem.* **2008**, *29*, 1859.
50. NAMD was developed by the Theoretical and Computational Biophysics Group in the Beckman Institute for Advanced Science and Technology at the University of Illinois at Urbana-Champaign."
51. Bot, G.; Blake, A. D.; Li, S.; Reisine, T. J. *Neurochem.* **1998**, *70*, 358.
52. Surratt, Christopher K.; Johnson, Peter S.; Moriwaki, Akiyoshi; Seidleck, Brian K.; Blaschak, Carrie J.; Wang, Jia Bei; Uhl, George R. *J. Biochem. Chem.* **1994**, *269*, 20548.
53. Al-Hasani, Ream; Bruchas, Michael R. *Anesthesiology* **2011**, *115*, 1363.
54. Fenalti, G.; Zatspein, Nadia A.; Betti, Cecilia; Giguere, Patrick; Han, Gye Won; Ishchenko, Andrii; Liu, Wei; Guillemin, Karel; Zhang, Haitao; James, Daniel; Wang, Dingjie; Weierstall, Uwe; Spence, John C. H.; Boutet, Sébastien; Messerschmidt, Marc; Williams, Garth J.; Gati, Cornelius; Yefanov, Oleksandr M.; White, Thomas A.; Oberthuer, Dominik; Metz, Markus; Yoon, Chun Hong; Barty, Anton; Chapman, Henry N.; Basu, Shibom; Coe, Jesse; Conrad, Chelsie E.; Fromme, Raimund; Fromme, Petra; Tourwé, Dirk; Schiller, Peter W.; Roth, Bryan L.; Ballet, Steven; Katritch, Vsevolod; Stevens, Raymond C.; Cherezov, Vadim *Nat. Struct. Mol. Biol.* **2015**, *22*, 265.